ACCEPTED VERSION

http://hdl.handle.net/2440/69613

Synthesis and coordination chemistry of 2-(di-2-pyridylamino)pyrimidine; structural aspects of spin crossover in an Fe(II) complex

Rachel S. Crees,[A] Boujemma Moubaraki,[B] Keith S. Murray,[B] and Christopher J. Sumby[A,C]

[A] School of Chemistry and Physics, University of Adelaide, Adelaide, SA 5005, Australia.

[B] School of Chemistry, Monash University, Clayton, Vic. 3800, Australia.

[C] Corresponding author. Email: christopher.sumby@adelaide.edu.au

Dedicated to Allan White on his 75th birthday – for demonstrating the significance of structural studies to spin crossover chemistry

Abstract

2-(Di-2-pyridylamino)pyrimidine (**L**), a potentially ditopic tetradentate ligand, was synthesized from commercially available di-2-pyridylamine and 2-chloropyrimidine. Despite being capable of bridging two metal atoms with bidentate chelation of both metal centres, **L** prefers to chelate or bridge through the more basic pyridyl donors of the di-2-pyridylamine moiety. Mononuclear *trans*-[Fe(NCS)$_2$(**L**)$_2$] and [Cu(**L**)$_2$(H$_2$O)](BF$_4$)$_2$·H$_2$O complexes, and a discrete [Ag$_2$(**L**)$_4$](PF$_6$)$_2$ metallo-macrocycle were isolated and structurally characterized by X-ray crystallography. A mononuclear palladium complex [PdCl$_2$(**L**)]·(solvate), where solvate = ½H$_2$O or CH$_2$Cl$_2$, was also readily obtained in 71% yield. One example of the ligand acting as a bis(bidentate) bridging ligand was observed in a dinuclear [(PdCl$_2$)$_2$(**L**)]·¾H$_2$O complex that was obtained only in very low yield (*ca.* 3%) from the reaction that produced [PdCl$_2$(**L**)]·½H$_2$O. *trans*-[Fe(NCS)$_2$(**L**)$_2$] undergoes a temperature dependent HS-LS (HS = high spin; LS = low spin) crossover at *ca.* 205 K that was

observed by X-ray crystallography and magnetic measurements and attempts were made to understand the structural basis of this process. Despite efforts to isolate examples of **L** bridging two iron(II) centres, only the mononuclear *trans*-[Fe(NCS)$_2$(**L**)$_2$] species could be obtained.

Introduction

The magnetic properties of multinuclear transition metal complexes have received sustained attention due to interest in their fundamental spin-crossover (SCO) properties and potential applications as switches, for memory storage, and as sensors, for example.[1-8] In this regard, multinuclear transition metal complexes in which the bridging ligands have the potential to chelate all metal centres engenders materials with greater stability, potentially enhanced metal–metal interaction, and improved magnetic switching behaviour.[3, 5, 7] Improved cooperativity in switching can result in improved hysteretic behaviour and, from a device perspective, a more useful SCO system.[3, 5, 7] An example of such a chelating ligand, 2,2'-bipyrimidine (bpym), has been the subject of significant investigation and has been shown to form complexes with short metal–metal distances.[9] For example, Real's classic Fe(II) dinuclear SCO complexes,[10, 11] [{Fe(bpym)(NCE)$_2$}$_2$-μ-bpym] (E = S, Se) utilize bpym to facilitate spin coupling in this SCO system with short metal–metal separations of ~5.5 Å.

Bridging ligands possessing 2,2'-bipyridine (**bpy**) and 1,10-phenanthroline units (**phen**),[12] di-2-pyridylmethane (**dpm**),[13, 14] and di-2-pyridylamine (**dpa**)[13] chelating motifs, Figure 1(a), for facilitating strong metal–metal interactions within multinuclear complexes have been studied. In the context of systems for spin crossover, the use of di-2-pyridylamine as a chelating motif has attracted considerable attention.[15-22] Kepert and Murray observed either a one-step or a two-step full spin crossover for dinuclear iron(II) complexes of 2,5-bis(di-2-pyridylamino)pyridine (**1**), with spin states HS–HS, HS–LS and LS–LS (HS: high spin, LS: low spin) for the two iron(II) centres at the three plateau temperatures in the two-step case.[15, 16] The incorporation of pyrimidine as a core in such ligands in the form of 4,6-bis(di-2-pyridylamino)pyrimidine (**2**) and its application in a SCO system has been reported,[17, 18]. Triazine derivatives have also been much studied in respect of SCO chemistry;[23, 24] some work on compounds containing two di-2-pyridylamine arms has been reported (**3**),[19] as has work on the tritopic version (**4**).[20-22]
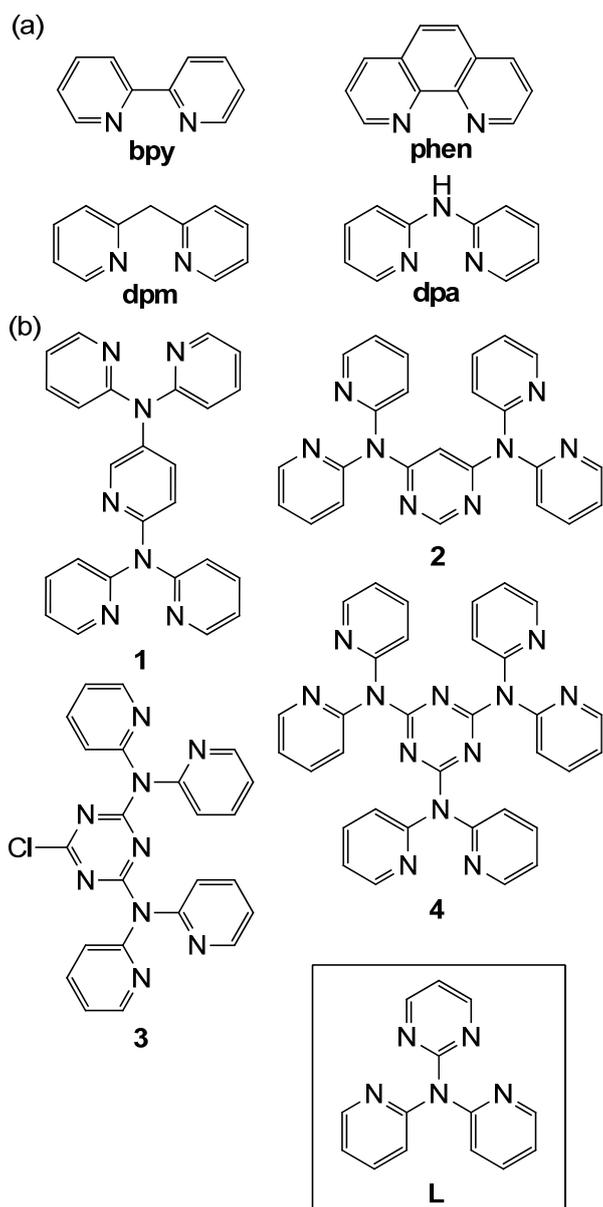
Figure 1. (a) Commonly encountered heterocyclic chelating moieties used in bridging ligands. (b) The structures of 2,5-bis(di-2-pyridylamino)pyridine (**1**), 4,6-bis(di-2-pyridylamino)pyrimidine (**2**), 2-chloro[4,6-(di-2-pyridylamino)]-1,3,5-triazine (**3**), 2,4,6-tris(di-2-pyridylamino)-1,3,5-triazine (**4**) and 2-(di-2-pyridylamino)pyrimidine (**L**).

We proposed that one of the simplest bis(bidentate) bridging ligands in this class would be 2-(di-2-pyridylamino)pyrimidine (**L**) in which two metal centres would be separated by a pyrimidine ring, akin to Real's 2,2'-bipyrimidine SCO complexes.[10, 11] Herein, we report the synthesis of **L** from 2-chloropyrimidine and di-2-pyridylamine, and the synthesis of mononuclear *trans*-[Fe(NCS)$_2$(**L**)$_2$],

[Cu(**L**)$_2$(H$_2$O)](BF$_4$)$_2$·H$_2$O, [PdCl$_2$(**L**)] ·(solvate), where solvate = ½H$_2$O or CH$_2$Cl$_2$, and dinuclear [(PdCl$_2$)$_2$(**L**)]·¾H$_2$O and [Ag$_2$(L)$_4$](PF$_6$)$_2$ complexes. We also describe the temperature dependent HS-LS crossover for *trans*-[Fe(NCS)$_2$(**L**)$_2$] by X-ray crystallography and magnetic measurements.

Results & Discussion

Ligand Synthesis

The method of Mosny and Crabtree[25] for the synthesis of tri-2-pyridylamine was adapted for the synthesis of 2-(di-2-pyridylamino)pyrimidine (**L**). Thus, reaction of di-2-pyridylamine with 2-chloropyrimidine in refluxing mesitylene provided low yields of the desired product **L** (typically 10-15%). Due to the greater availability of 2-chloropyrimidine, we tried to improve the yield of **L** by using a reasonable excess of this reagent (four equivalents) as reported;[25] unfortunately, this resulted in a mixture of product and residual 2-chloropyrimidine that was extremely difficult to purify. Limited attempts at synthesising **L** by Buchwald-Hartwig amination chemistry starting from 2-aminopyrimidine and 2-bromopyridine were unsuccessful despite this generally being a viable route to di-2-pyridylamine containing bridging ligands.[13] Thus, we returned to our original reaction conditions, which were exploited to produce sufficient quantities of the **L** for characterization and subsequent investigation of its coordination chemistry.

Synthesis, structures, and properties of trans-[Fe(NCS)₂(L)₂] 5

Among the first compounds we attempted to synthesize were dinuclear and polymeric iron(II) complexes of **L** from Fe(ClO$_4$)$_2$·6H$_2$O (Scheme 1). This was initially attempted by reacting Fe(ClO$_4$)$_2$·6H$_2$O and **L** in a 2:1 or 1:1 ratio in the presence of excess KSCN. In both cases the main product isolated was *trans*-[Fe(NCS)$_2$(**L**)$_2$] (**5**), where **L** acts as a simple chelating ligand, and not the desired dinuclear and polymeric iron(II) complexes. As reported herein (Scheme 1), complex **5** could be prepared directly by undertaking the reaction of **L** with Fe(ClO$_4$)$_2$·6H$_2$O using a slightly greater than 2-fold excess of **L**, which gave yellow-brown crystals in 37% yield. The IR spectrum

confirmed the presence of **L**, with characteristic bands at 1600, 1558, 1465, and 1402 cm^{-1} corresponding to the ligand, while the N-bound thiocyanate anions were established by observation of the C≡N stretch at 2054 cm^{-1},[17] that is consistent with a high spin complex. The microanalysis data matched the calculated values for *trans*-[Fe(NCS)$_2$(**L**)$_2$] **5**. The formulation of the complex was further supported by electrospray mass spectrometry (ES-MS) that revealed an ion with *m/z* = 611.8, consistent with [Fe(NCS)$_2$(**L**)$_2$]$^+$.
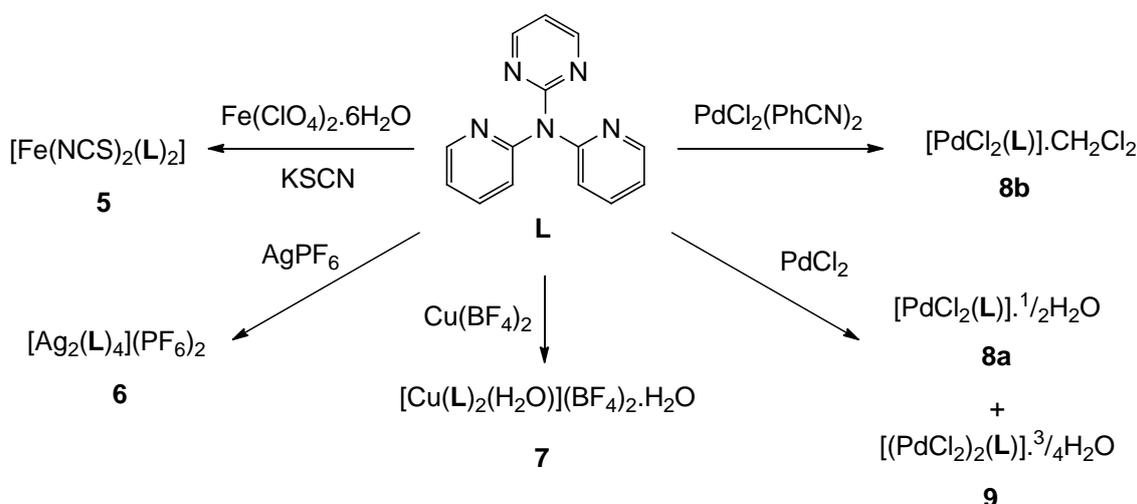

Scheme 1.

Crystal Structures of trans-[Fe(NCS)$_2$(L)$_2$] 5 at 150 and 293 K

Mounting crystals of **5** on the diffractometer at 150 K led to a rapid darkening of the yellow crystals consistent with a HS-LS SCO. Thus, data collections on *trans*-[Fe(NCS)$_2$(**L**)$_2$] were undertaken at room temperature and 150 K. Variable temperature unit cell determinations were also carried out to ascertain the onset of the SCO. At all temperatures studied, compound **5** crystallises in the triclinic space group *P*-1 with half the molecule (one ligand, one thiocyanate anion and half an iron(II) centre) in the asymmetric unit. The iron atom is located on a centre of inversion. In the room temperature form of the structure (**5RT**), Figure 2(a), the Fe-N bond lengths are in the range 2.0981(17) – 2.2277(14) Å. These are consistent with the high spin form of Fe(II) with six N-donor ligands (typical Fe-N bond length *ca*. 2.1 Å).[1, 26] In the room temperature form the N-Fe-N angle

6

of the di-2-pyridylamine moiety is more acute (81.99(6)° vs 86.52(5)° for **5**LT), as a consequence of the longer bond lengths required by the high spin iron(II) centre.
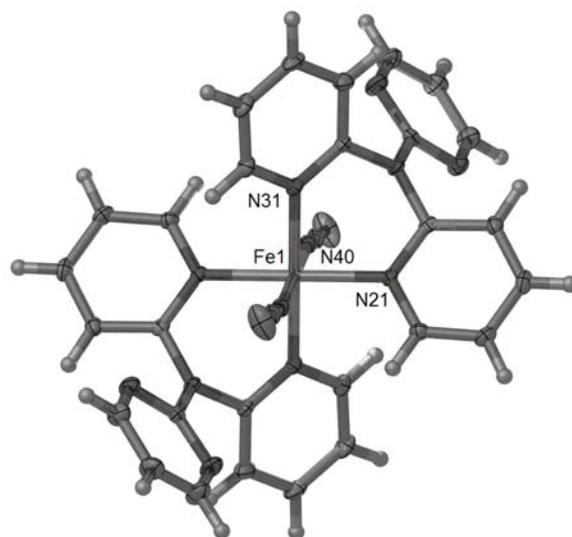
(a)
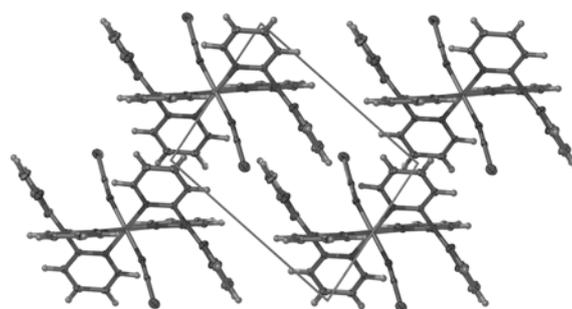
(b)

Figure 2. (a) A view of the low temperature, low-spin form of *trans*-[Fe(NCS)$_2$(**L**)$_2$] and (b) the packing of this complex, viewed down the *b*-axis. Selected bond lengths (Å) and angles (°): **5**RT, Fe1-N21 2.1971(15), Fe1-N31 2.2277(14), Fe1-N40 2.0981(17), N40-Fe1-N21 90.34(6), N40-Fe1-N31 92.12(6), N21-Fe1-N31 81.99(6); **5**LT, Fe1-N21 1.9873(13), Fe1-N31 1.9927(13), Fe1-N40 1.9503(14), N40-Fe1-N21 91.22(5), N40-Fe1-N31 92.54(5), N21-Fe1-N31 86.52(5).

In the low temperature (150 K) form of *trans*-[Fe(NCS)$_2$(**L**)$_2$], Figure 2(b), the Fe-N bond lengths range from 1.9503(14) to 1.9927(13) Å and, as expected, are considerably (0.14 – 0.23 Å) shorter than those observed in the room temperature structure. Typical Fe-N bond lengths for a LS iron(II) complex are *ca.* 1.95 Å.[1, 26] The most significant contraction in bond lengths occurs for the pyridyl donors of **L**, consistent with the major contraction in the unit cell parameters occurring along the *a*-axis. In HS *trans*-[Fe(NCS)$_2$(**L**)$_2$] the *a*-axis length is 8.63 Å and this contracts to 8.35 Å at 150 K, with the onset of the contraction occurring around 205 K. Aside from the shorter bond lengths, the low-spin form is isostructural with the high-spin structure.

Unit cell determinations on **5** were undertaken at multiple temperatures cycling from 280 K to 150 K and then warming the sample back to 280 K. We also determined the unit cell at higher temperatures but this just revealed additional minor thermally induced expansion of the unit cell parameters. Throughout the entire experiment, which was repeated on several crystals, the structure maintained the same unit cell (Figure 3). The *a*-axis undergoes a *ca.* 0.3 Å contraction during the SCO, while the *c*-axis length is slightly lengthened as a consequence of the HS-LS SCO (elongation of 0.1 Å). The *b*-axis remains essentially constant across the entire temperature range, although during the SCO (at *ca.* 205 K) there is a slight elongation presumably to accommodate the structural reorganisation. The contraction of the *a*- axis relates to a shortening of the pyridyl-N bonds to the iron(II) centre, while the slight elongation of the *c*-axis is a consequence of the change in the conformation of the chelate ring brought about by the shortening of the Fe-N bonds. The unit cell volume change, from HS to LS, was 4.7%, typical of such a spin transition.[1, 26]
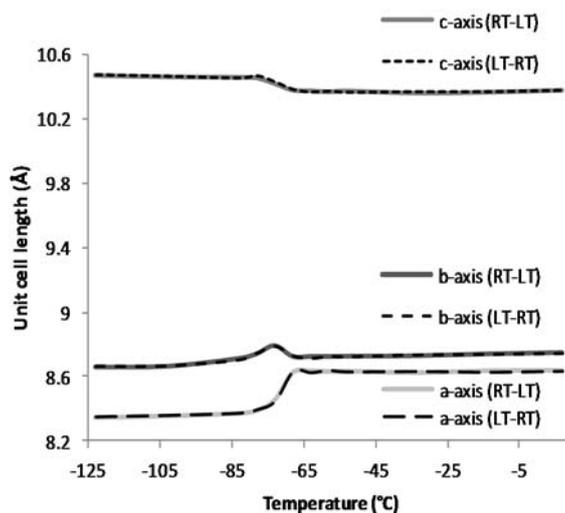
Figure 3. The unit cell lengths for **5** collected at multiple temperatures from 150 – 280 K (-123 – 7 °C). This graph shows the results for an individual crystal cooled from 280 K down to 150 K and warmed back to 280 K.

*Magnetism of trans-[Fe(NCS)$_2$(**L**)$_2$] **5***

In Figure 4, we see that the $\chi_M T$ values remain constant at 3.5 cm^3 mol^{-1} K between 280 and 205 K, a value typical of HS Fe^{II} (μ_{eff} = 5.29 μ_B) and then show an abrupt HS-LS spin transition at $T_{1/2}$ of 205 K before leveling off below ~150 K to a LS value of 0.05 cm^3 mol^{-1} K, the latter arising from second order Zeeman effects in the $^1A_{1g}$ state. Heating and cooling showed essentially zero thermal hysteresis, in agreement with the variable temperature crystallographic data (*vide supra*). Comparisons to some recent examples of *bis*-dipyridylamino chelates show that the *cis* derivative [Fe(NCS)$_2$(DDE)$_2$, where DDE = N^2,N^2,N^4,N^4-tetraethyl-N^6,N^6-di(pyridin-2-yl)-1,3,5-triazine-2,4,6-triamine,[23] a ligand with a diethylamino-substituted-triazine 'tails', has the same $T_{1/2}$ value and no hysteresis, but the transition is less abrupt, i.e. less cooperativity. A polymorph of *trans*-[Fe(NCS)$_2$(DBB)$_2$, where DBB = N^2,N^2,N^4,N^4-tetrabenzyl-N^6,N^6-di(pyridin-2-yl)-1,3,5-triazine-2,4,6-triamine, now containing dibenzylamino tails, shows a slightly less abrupt, non-hysteretic spin transition than does **5**, with $T_{1/2}$ = 170 K, while the other polymorph showed a gradual transition, with $T_{1/2}$ ~ 300 K.[24]

9

Detailed comparisons of packing features (π-stacking, H-bonding, chemical pressure, etc.), as well as of Fe(II) coordination spheres, were made for the DDE and DBB compounds to try and elucidate reasons for differences in $T_{1/2}$ and in cooperativity in comparison to **5**. This was of limited success since most such interactions play a part. In compound **5** the most prominent intermolecular interactions are edge-to-face π-stacking interactions[27] and weak C-H···S hydrogen bonds involving the acidic H4/H6 hydrogen atoms of **L** and the non-coordinated sulfur atoms of the thiocyanate ligands (C-H···S: **5LT**, d_{H-S} = 2.86, D_{CS} = 3.57 Å, $angle_{C-H···S}$ = 133.0°; **5RT**, d_{H-S} = 2.92, D_{CS} = 3.59 Å, $angle_{C-H···S}$ = 128.0°).[28, 29] Each molecule of **5** makes four such weak hydrogen bonds to two different molecules of **5** within the structure, while edge-to-face π-stacking interactions provide connections to four other molecules. Fe(II) complexes of DDE and DBB lack such acidic hydrogen atoms for forming hydrogen bonds of the type observed here for **5.**
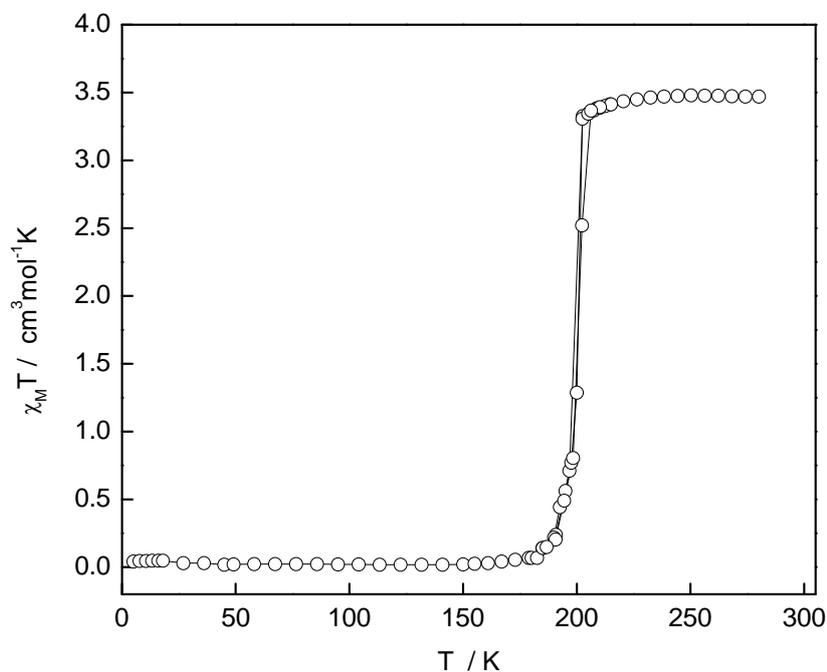

Figure 4. Plot of $\chi_M T$ vs. T for complex **5**. The solid line just joins the points.

Coordination chemistry with Ag(I), Cu(II) and Pd(II)

As a consequence of being unable to obtain dinuclear or polymeric iron(II) complexes in which **L** acted as a bridging ligand, we set out to form complexes with other metal salts that might demonstrate the desired coordination mode and provide structural insight into the problems associated with tetradentate coordination of **L** (Scheme 1). Reaction of methanol solutions of **L** and AgPF$_6$ gave a colourless solution that yielded block-shaped crystals of [Ag$_2$(**L**)$_4$](PF$_6$)$_2$ (**6**) in 79% yield by slow evaporation. The IR spectrum confirmed the presence of **L**, with characteristic bands at 1586, 1561 and 1406 cm^{-1} corresponding to the ligand, and a very strong band at 834 cm^{-1} consistent with the P-F stretch of the hexafluorophosphate anion. Dissolution of the crystals in CD$_3$CN gave a ^{1}H NMR spectrum at room temperature with one chemical environment for **L**, inconsistent with the single crystal structure, where the di-pyridylamine moieties of the four ligands are found to either bridge or chelate the silver(I) centres. This was confirmed by variable temperature NMR experiments on **6** (to -30°C) which could not resolve individual signals for the bridging and chelating modes of **L**. This may be a consequence of an exchange process that is rapid on the NMR timescale (at room temperature and -30°C) or due to dissociation of **6** to give a mononuclear complex [Ag(**L**)$_2$]PF$_6$ in solution. The second proposal is supported by ES-MS for **6**, dissolved in CH$_3$CN, that revealed molecular ions at *m/z* 604.8 and 606.9 corresponding to [^{107}Ag(**L**)$_2$]$^+$ and [^{109}Ag(**L**)$_2$]$^+$, respectively. The ions [^{107}Ag(**L**)]$^+$ and [^{109}Ag(**L**)]$^+$ were also observed but there was no evidence for the desired dinuclear [Ag$_2$(**L**)$_4$]$^{2+}$ complex. The ^{1}H NMR spectrum of dissolved **6** shows minor coordination induced downfield shifts for the pyridine hydrogen atoms (Figure SI 1) consistent with chelation of the silver(I) cation by the di-pyridylamine moiety of at least one ligand. The pyrimidine H4 proton is unaffected by coordination and the signal for pyrimidine H3/H5 moves slightly upfield.

X-ray crystallography revealed that **6** is a dimetallo-macrocycle in which the two silver centres are bridged by the di-2-pyridylamine moieties of two molecules of **L**, Figure 5(a). Compound **6**

crystallizes in the triclinic space group *P*-1 with one silver atom, two ligand molecules and a disordered hexafluorophosphate in the asymmetric unit. The silver centre adopts a distorted tetrahedral geometry that is coordinated by one ligand molecule in a chelating mode and two others in the bridging mode mentioned above. The bridging of the two silver centres as observed here for **L** has been previously seen for other ligands containing a di-2-pyridylamine moiety.[30, 31] As a consequence, the silver centres are separated by 3.42(1) Å, consistent with the type of coordination motif in previous work.[30, 31] The pyrimidine ring of **L** is not involved in coordination of the silver but does form intra- and intermolecular π-stacking interactions with the coordinated pyridine rings of the same metallo-macrocycle and the pyrimidine rings of adjacent metallo-macrocycles, Figure 5(b).
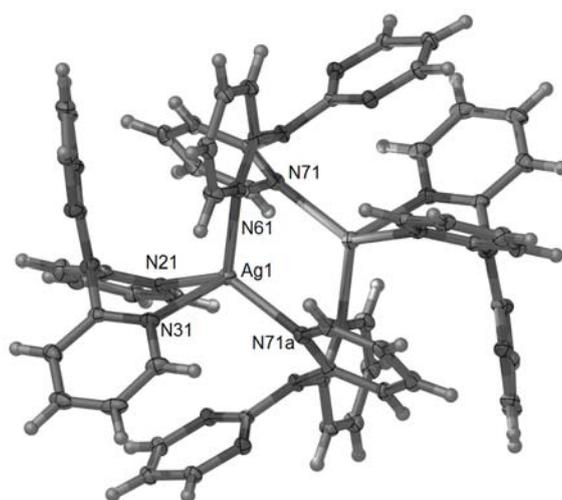
(a)
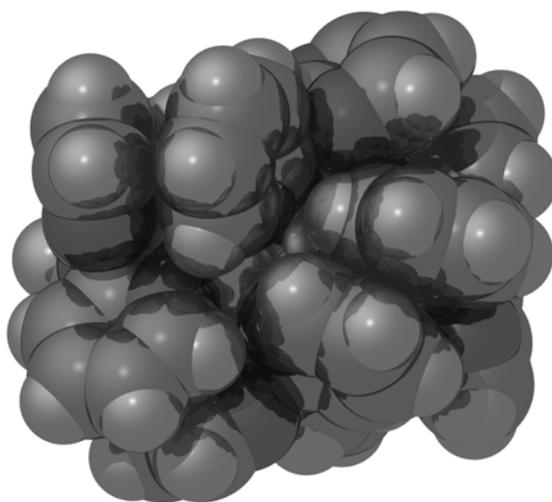
(b)

Figure 5. A perspective view of complex **6** showing the chelating and bridging modes of **L**; (a) an ellipsoid plot at 50% probability level and (b) a space-filling representation of the discrete complex. The disordered hexafluorophosphate anions are not shown. Selected bond lengths (Å) and angles (°): Ag1-N71a 2.3149(13), Ag1-N21 2.3207(12), Ag1-N61 2.3747(12), Ag1-N31 2.4859(13), N71a-Ag1-N21 132.17(4), N71a-Ag1-N61 105.39(4), N21-Ag1-N61 122.05(4), N71a-Ag1-N31 97.23(4), N21-Ag1-N31 83.72(4), N61-Ag1-N31 96.92(4). Symmetry code -X, -Y, 2-Z.

A copper(II) complex, $[Cu(L)_2(H_2O)](BF_4)_2 \cdot H_2O$ (**7**), was also obtained in which the copper centre was chelated by two molecules of **L**; in both molecules only the pyridyl donors are involved in coordination. Simply combining of methanol solutions of **L** and $Cu(BF_4)_2$ gave blue crystals of **7** in 26% yield after a few days; this reaction was conducted with several different starting stoichiometries but the major isolated product was always the CuL_2 complex. FTIR spectroscopy confirmed the presence of **L** (stretches 1603, 1562, and 1408 cm^{-1}), water (3445 cm^{-1}) and a B–F stretch at 1053 cm^{-1} established the tetrafluoroborate anion. In the crystal structure of compound **7**, the copper(II) centre has a geometry best described as distorted square pyramidal chelated by two molecules of **L** in the basal plane, while a water ligand in the axial position completes the coordination sphere. The τ parameter for Cu1 is 0.34.[32] As noted, the pyrimidine rings of **L** are

not involved in coordinating to the copper atom and instead are involved in an intramolecular π-stacking interaction (Figure 6). A very similar coordination environment is observed for a copper(II) complex of 1,4-bis(6-[di-2-pyridylamino]-4-pyrimidyloxy)benzene whereby the copper centre is coordinated by two di-2-pyridylamine chelating moieties and the fifth coordination site filled by a solvent molecule; in that case a second copper is also coordinated by the ligand.[33]
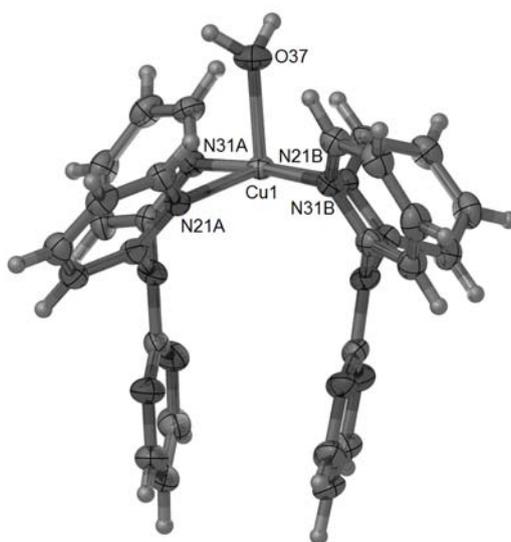
Figure 6. A perspective view of complex **7** showing the chelating coordination mode of **L** (non-coordinated solvate molecules and the tetrafluoroborate anions are omitted for clarity). Selected bond lengths (Å) and angles (°): Cu1-N31A 2.015(3), Cu1-N31B 2.018(3), Cu1-N21B 2.028(3), Cu1-N21A 2.040(3), Cu1-O37 2.128(3), N31A-Cu1-N31B 173.35(12), N21B-Cu1-N21A 152.90(12).

We finally turned to the predictable coordination requirements of palladium(II) chloride in an effort to obtain an example of **L** acting as a bis(bidentate) ligand. Firstly, **8a** was obtained in 71% yield as a pale yellow-orange precipitate by reacting a methanol solution of **L** with a dilute hydrochloric acid solution of $PdCl_2$ in a M:L ratio of 2.15:1. The precipitate was readily identified as a mononuclear complex [$PdCl_2$(**L**)]·½H_2O (**8a**) by a combination of FT-IR spectroscopy, ^{1}H NMR spectroscopy, ES-MS and elemental analysis. The ^{1}H NMR spectrum of **8a** shows one set of

pyridyl resonances, consistent with a mononuclear complex coordinated only by the pyridyl donors. In addition, more significant downfield shifts of the resonances of the pyridyl protons were observed (see Figure SI 2) confirming the coordination mode. This was further supported by the isolation of [PdCl$_2$(**L**)]·CH$_2$Cl$_2$ (**8b**) in 82% yield. Complex **8b** was obtained by layering a dichloromethane solution of **L** with THF and then a toluene solution of [PdCl$_2$(PhCN)$_2$], which gave, over a few days, a mixture of yellow rod-shaped crystals and yellow precipitate. An X-ray crystal structure obtained from the yellow rod-shaped crystals confirmed the mononuclear nature of the complex **8b**, as anticipated from NMR studies of both solvates (see Figure SI 2). Despite the use of an Pd:**L** ratio of 2.15:1 for both the reactions, the major product (71% and 82% yield, respectively) was the mononuclear complex [PdCl$_2$(**L**)]. Eventually, leaving the aqueous-methanol filtrate of the reaction used to produce **8a** to slowly evaporate allowed us to identify a minor amount (<3% isolated yield) of a dinuclear complex, [(PdCl$_2$)$_2$(μ$_2$-**L**)]·¾H$_2$O (**9**), as yellow crystals. This complex was obtained from a solution containing Pd:**L** in an approximate 5:1 stoichiometry, indicating that a large excess of metal is required to force this ligand to bridge metal ions in the desired bis(bidentate) mode.

Further confirmation of the coordination mode in both the mononuclear and dinuclear palladium complexes came from X-ray crystallography. Complex **8b** crystallizes in the monoclinic space group *P*2$_1$/*n* with one complete molecule in the asymmetric unit, Figure 7(a). The palladium has the expected square planar geometry with bond lengths typical of this donor set and chelation by the pyridyl nitrogen atoms only, as established by solution studies. Complex **9** also has a square planar coordination geometry at both palladium centres, which possess almost identical bond lengths and angles to the palladium centre in **8b**, Figure 7(b). [(PdCl$_2$)$_2$(μ$_2$-**L**)]·¾H$_2$O crystallizes in the monoclinic space group *C*2/*c* with a complete molecule in the asymmetric unit. To accommodate the bis(bidentate) chelating motif in **9**, the di-2-pyridylamine moiety is twisted by approximately 50° out of the plane of the pyrimidine ring; by comparison this twist is negligible (*ca.* 4°) in

complex **8b**. This twisted conformation allows the two six membered chelate rings to adopt the preferred boat conformation and achieve the tetradentate coordination mode.[13]
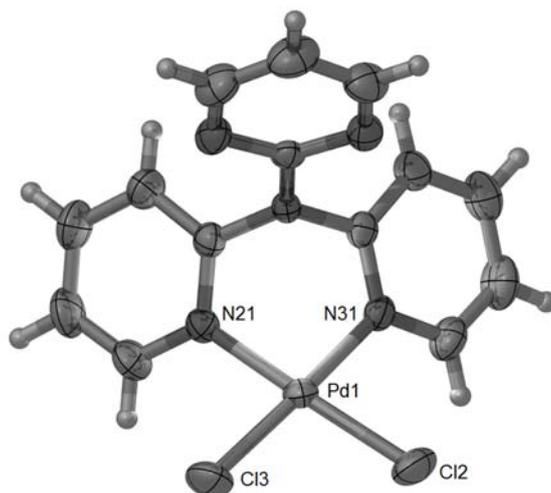
(a)
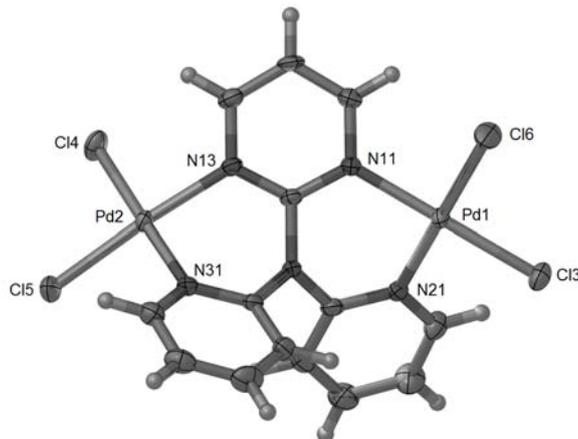
(b)

Figure 7. (a) A perspective view of complex **8b** showing the chelating coordination mode of **L** in the mononuclear complex (the dichloromethane solvate molecule has been omitted). Selected bond lengths (Å): Pd1-N21 2.030(3), Pd1-N31 2.039(3), Pd1-Cl3 2.2724(10), Pd1-Cl2 2.2844(9). (b) A perspective view of complex **9** showing the bis(bidentate) coordination mode of **L** in [(PdCl$_2$)$_2$(μ_2-**L**)]·¾H$_2$O (the partially occupied water solvate molecules have been omitted).

Selected bond lengths (Å) and angles (°): Pd1-N21 2.028(3), Pd1-N11 2.047(3), Pd1-Cl3 2.2803(13), Pd1-Cl6 2.2855(10), Pd2-N31 2.025(3), Pd2-N13 2.040(3), Pd2-Cl4 2.2796(11), Pd2-Cl5 2.2857(10).

Conclusion

A new heterocyclic ligand, 2-(di-2-pyridylamino)pyrimidine **L**, was synthesised from commercially available starting materials in a single step. By analogy to related work, this compound was proposed to be capable of three main coordination modes; chelating and bridging through the dpa moiety only, or a tetradentate bis(bidentate) bridging mode involving all four donors, see Figure 8. All three modes were observed in this work. As is typical for these dpa chelating units, the tertiary nitrogen atom is planar and this necessitates significant twisting of **L** in the one dinuclear complex, [(PdCl₂)₂(L)] **9**, that was obtained with a bis(bidentate) bridging coordination mode.
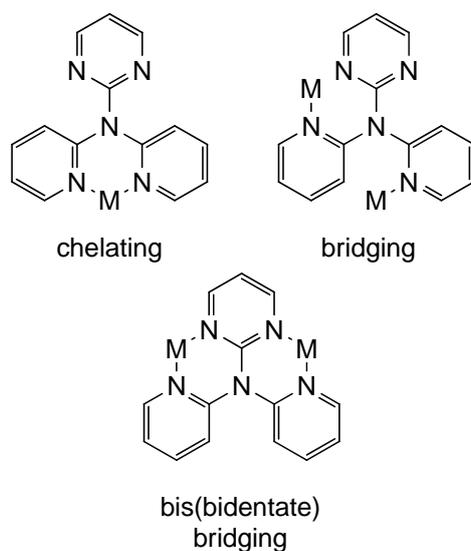
Figure 8. The coordination modes encountered for **L** in this study.

In spite of being capable of bridging two metal atoms with bidentate chelation of both metal centres, **L** prefers to chelate or bridge through the more basic di-2-pyridylamine moiety. Mononuclear *trans*-[Fe(NCS)₂(**L**)₂] (**5**) and [Cu(**L**)₂(H₂O)](BF₄)₂·H₂O (**7**) complexes, and a discrete [Ag₂(**L**)₄](PF₆)₂ metallomacrocycle (**6**) were isolated and structurally characterized by X-ray

crystallography. A mononuclear palladium complex [PdCl$_2$(**L**)] was also readily obtained in 71 and 82% yield (water, **8a**, and dichloromethane solvates, **8b**, respectively). Furthermore, one example of the ligand acting as a bis(bidentate) bridging ligand was observed in a dinuclear [(PdCl$_2$)$_2$(L)] **9** that was obtained in very low yield (*ca.* 3%). This preference for the chelating and bridging coordination modes involving the dpa moiety only is a consequence of the basicity of the nitrogen donors; the pyrimidine nitrogens are considerable weaker bases than the pyridine nitrogens due to the electron withdrawing effect of the second ring nitrogen atom (pyridine pK_a 5.2 vs pyrimidine pK_a 1.3).

Complex **5** undergoes a temperature dependent HS-LS crossover at 205 K that was observed by X-ray crystallography and, as an abrupt non-hysteretic spin transition, by magnetic measurements. Variable temperature unit cell determinations undertaken on selected crystals of **5** revealed that the HS and LS forms have that same triclinic unit cell and that the *a*-axis undergoes a *ca.* 0.3 Å contraction as a consequence of the HS-LS transition. Analysis of the single crystal X-ray structures of both forms of **5** identified that the contraction of the *a*-axis relates predominantly to a shortening of the pyridyl-N bonds to the iron(II) centre. Attempts to relate crystal packing interactions to the cooperativity between SCO molecules, as indicated by the abrupt spin change, showed weak C-H···S hydrogen bonds and π-stacking interactions were the dominant intermolecular forces involved in the crystal packing of **5**. We note, with gratitude, that Martin and White paved the way, in the 1960's, for structure-magnetism correlations in mononuclear *d*-block SCO species.[34] Notwithstanding the efforts already made to isolate examples of **L** bridging two iron(II) centres, we are continuing to investigate the synthesis of other Fe(II) complexes of **L** that may display the desired bridging mode and concomitantly interesting magnetic properties.

Experimental

General experimental

Melting points were measured on a Gallenkamp melting point apparatus and are uncorrected. Elemental analyses were performed by the Campbell Microanalytical Laboratory at the University of Otago. Infrared spectra were collected on a Perkin Elmer 100S Infrared spectrometer in Universal ATR mode. NMR spectra were recorded on Gemini 300 MHz NMR spectrometer at 23 °C using a 5 mm probe. ^{1}H NMR spectra recorded in CDCl$_3$ were referenced relative to the internal standard Me$_4$Si; ^{1}H NMR spectra recorded in DMSO-d$_6$ were referenced to the solvent peak, 2.6 ppm. Electrospray (ES) mass spectra were recorded using a Finnigan LCQ mass spectrometer. Unless otherwise stated, all chemicals were obtained from commercial sources and used as received. [PdCl$_2$(PhCN)$_2$][35] was prepared according to the method described in the literature. Magnetic susceptibilities were measured on a Quantum Design MPMS XL7 Squid instrument that was calibrated against a Pd pellet of accurately known susceptibility value (Quantum Design Inc.). The 20 mg sample of **5** was dispersed in a Vaseline mull to prevent any 'torquing' of crystallites that can occur in the orbitally degenerate HS state.

Synthesis

Synthesis of 2-(di-2-pyridylamino)pyrimidine (L). Di-2-pyridylamine (2.05 g, 0.0120 mol), 2-chloropyrimidine (1.65 g, 0.0144 mol), copper powder (0.82 g), potassium iodide (0.47 g), and potassium carbonate (4.02 g) were suspended in mesitylene (20 mL). The mixture was heated at 160 °C for 96 hours, cooled to room temperature and filtered through celite. The celite pad was washed with dichloromethane (3 × 20 mL) and the organic extracts combined with the mesitylene. The solvent was removed by distillation under high vacuum to give an oily solid that was recrystallised from ethyl acetate and hexane to give a pale yellow solid (0.35 g, 12%). Mp 109 – 110 °C. Anal. found: C, 67.66; H, 4.40; N, 27.84. C$_{14}$H$_{11}$N$_5$ requires C, 67.44; H, 4.46; N, 28.10%; ^{1}H NMR (300 MHz; CDCl$_3$; Me$_4$Si) δ = 6.87 (1H, t, $^3J_{HH}$ = 4.8 Hz, pymH4), 7.14 (2H, dd, $^3J_{HH}$ = 4.9 and 7.4 Hz, pyH5), 7.37 (2H, d, $^3J_{HH}$ = 8.1 Hz, pyH3), 7.74 (2H, dd, $^3J_{HH}$ = 8.1 and 7.4 Hz pyH4), 8.46 (2H, d, $^3J_{HH}$ = 4.9 Hz pyH6), 8.48 (2H, d, $^3J_{HH}$ = 4.8 Hz pymH3/H5). ^{1}H NMR (300

MHz; CD$_3$CN; Me$_4$Si) δ = 6.99 (1H, t, $^3J_{HH}$ = 4.8 Hz, pymH4), 7.16 (2H, dd, $^3J_{HH}$ = 4.9 and 7.4 Hz, pyH5), 7.33 (2H, d, $^3J_{HH}$ = 8.1 Hz, pyH3), 7.76 (2H, dd, $^3J_{HH}$ = 8.1 and 7.4 Hz pyH4), 8.32 (2H, d, $^3J_{HH}$ = 4.9 Hz pyH6), 8.45 (2H, d, $^3J_{HH}$ = 4.8 Hz pymH3/H5). ^{1}H NMR (300 MHz; DMSO-d$_6$; Me$_4$Si) δ = 7.08 (1H, t, $^3J_{HH}$ = 4.7 Hz, pymH4), 7.19 (2H, dd, $^3J_{HH}$ = 4.9 and 7.4 Hz, pyH5), 7.32 (2H, d, $^3J_{HH}$ = 8.1 Hz, pyH3), 7.80 (2H, dd, $^3J_{HH}$ = 8.1 and 7.4 Hz pyH4), 8.31 (2H, d, $^3J_{HH}$ = 4.9 Hz pyH6), 8.52 (2H, d, $^3J_{HH}$ = 4.7 Hz pymH3/H5). ^{13}C NMR (75.1 MHz; CDCl$_3$; Me$_4$Si) δ = 115.61, 121.07, 121.35, 139.03, 148.11, 155.02, 158.25, 161.37. *m/z* (ES-MS) 250.1 (MH$^+$), 271.9 (MNa$^+$). Selected IR bands (neat, cm^{-1}): 3040 (w), 1584 (s), 1560 (s), 1462 (m), 1401 (s), 1322 (m), 783 (s).

[Fe(NCS)$_2$(L)$_2$] (5). A solution of L (45.1 mg, 0.181 mmol) dissolved in methanol (8 mL) was combined with a solution of Fe(ClO$_4$)$_2$·6H$_2$O (22.4 mg, 0.088 mmol) and KSCN (34 mg, excess) in methanol (12 mL) to give a purple-red solution. Over a period of weeks yellow rod-shaped crystals of **5** were obtained. These were collected by decanting the solvent, washing the crystals with two portions of cold methanol (2 x 5 mL) and diethyl ether (5 mL), and drying in air (21.6 mg, 37%). Mp 282 – 284 °C. Anal. found: C, 53.88; H, 3.20; N, 24.80. C$_{30}$H$_{22}$N$_{12}$S$_2$Fe requires C, 53.73; H, 3.31; N, 25.07%. Selected IR bands (ATR, cm^{-1}): 2054 (s, C≡N str.), 1600 (m), 1558 (s), 1465 (s), 1402 (s), 791 (s). *m/z* 611.8 ([Fe(NCS)(L)$_2$]$^+$, 100%). λ_{max}/nm: 450 (ε/M^{-1} cm^{-1} 337) in DMSO.

[Ag$_2$(L)$_4$](PF$_6$)$_2$ (6). A solution of L (25.2 mg. 0.10 mmol) in methanol (2 mL) and a solution of AgPF$_6$ (12.5 mg, 0.050 mmol) in methanol (2 mL) were combined and left to slowly evaporate. After one week, colourless block shaped crystals were obtained. These were collected by filtration, washed with diethyl ether and dried to give **6** (30.0 mg, 79%). Mp >170°C (dec.). Anal. found: C, 44.62; H, 2.90; N, 18.88. C$_{56}$H$_{44}$N$_{20}$F$_{12}$P$_2$Ag$_2$ requires C, 44.84; H, 2.96; N, 18.68%. Selected IR bands (ATR, cm^{-1}): 1586 (m), 1561 (m), 1406 (s), 1330 (w), 834 (vs, P-F str.). A sample of **6** was redissolved in CD$_3$CN: ^{1}H NMR (300 MHz; CD$_3$CN; Me$_4$Si) δ = 6.98 (1H, t, pymH4), 7.22 (2H, dd, pyH5), 7.40 (2H, d, pyH3), 7.81 (2H, dd, pyH4), 8.34 (2H, d, pyH6), 8.44 (2H, d, pymH3/H5).

m/z 356.1 ($[^{107}\text{Ag}(\textbf{L})]^+$, 6%), 358.1 ($[^{109}\text{Ag}(\textbf{L})]^+$, 7%), 560.9, 562.9, 604.8 ($[^{107}\text{Ag}(\textbf{L})_2]^+$, 100%), 606.9 ($[^{109}\text{Ag}(\textbf{L})_2]^+$, 92%).

[Cu(L)$_2$(H$_2$O)](BF$_4$)$_2$·H$_2$O (7). A solution of L (24.9 mg. 0.10 mmol) in methanol (3 mL) and a solution of Cu(BF$_4$)$_2$·xH$_2$O (11.9 mg, 0.050 mmol) in methanol (2 mL) were combined to give a blue-green solution and left to slowly evaporate. After a few days a blue crystals were obtained. These were collected by filtration, washed with methanol, then diethyl ether and dried to give **7** (10.1 mg, 26%). Mp 298 – 300 °C. Anal. found: C, 43.40; H, 2.99; N, 18.02. C$_{28}$H$_{26}$B$_2$N$_{10}$O$_2$F$_8$Cu requires C, 43.57; H, 3.40; N, 18.15%. Selected IR bands (ATR, cm^{-1}): 3445 (w), 3038 (w), 1603 (m), 1562 (m), 1408 (s), 1053 (s), 1027 (s), 791 (s). *m/z* 561.0 ($[^{63}\text{Cu}(\textbf{L})_2]^+$, 32%), 563.0 ($[^{65}\text{Cu}(\textbf{L})_2]^+$, 14%), 579.9 ($[^{63}\text{Cu}(\textbf{L})_2(\text{H}_2\text{O})]^+$, 100%), 581.9 ($[^{65}\text{Cu}(\textbf{L})_2(\text{H}_2\text{O})]^+$, 41%), 595.8, 597.8, 680.9 ($\{[^{63}\text{Cu}(\textbf{L})_2(\text{CH}_3\text{OH})](\text{BF}_4)\}^+$, 100%), 682.9 ($\{[^{65}\text{Cu}(\textbf{L})_2(\text{CH}_3\text{OH})](\text{BF}_4)\}^+$, 97%). λ_{max}/nm: 425 (sh.), 795 (ε/M^{-1} cm^{-1} 31) in DMSO.

[PdCl$_2$(L)]·(solvent) (solvent = ½H$_2$O, 8(½H$_2$O); solvent = CH$_2$Cl$_2$, 8(CH$_2$Cl$_2$)) and [(PdCl$_2$)$_2$(μ$_2$-L)]·¾H$_2$O (9). Method A: To a solution of L (24.9 mg, 0.100 mmol) dissolved in methanol (5 mL) was added a solution of PdCl$_2$ (38.2 mg, 0.215 mmol) dissolved in 2M HCl solution (5 mL). Immediately upon mixing a pale yellow-orange precipitate formed. This was collected by filtration, the solid washed with methanol and diethyl ether, and dried to give **8b** (31.0 mg, 71%). The orange filtrate was left to slowly evaporate yielding yellow crystals, which were collected, washed with methanol and diethyl ether, and dried to give [(PdCl$_2$)$_2$(μ$_2$-L)] (1.5 mg, <3%). [PdCl$_2$(L)]·½H$_2$O, **8a**: Mp >290 °C (dec.). Anal. found: C, 38.62; H, 2.50; N, 15.87. C$_{14}$H$_{12}$N$_5$O$_{0.5}$Cl$_2$Pd requires C, 38.60; H, 2.78; N, 16.08%. ^{1}H NMR (300 MHz; DMSO-d$_6$) δ = 7.29 (1H, t, pymH4), 7.69 (2H, dd, pyH5), 8.12 (2H, d, pyH3), 8.29 (2H, dd, pyH4), 8.68 (2H, d, pymH3/H5), 8.81 (2H, d, pyH6). Selected IR bands (ATR, cm^{-1}): 1598 (m), 1558 (m), 1481 (m), 1466 (m), 1402 (vs), 1362 (w), 1331 (w), 1294 (w), 814 (w), 754 (m). *m/z* 450.5

({[PdCl$_2$(**L**)]+Na}$^+$, 18%), 465.9 ({[PdCl$_2$(**L**)]+Na(H$_2$O)}$^+$, 5%), 818.9 ({[PdCl$_2$(**L**)][PdCl(**L**)]}$^+$, 100%), 876.5 ({[PdCl$_2$(**L**)]$_2$+Na}$^+$, 36%), 892.4 ({[PdCl$_2$(**L**)]+Na(H$_2$O)}$^+$, 25%). λ_{max}/nm: 420 (sh.) in DMSO. [(PdCl$_2$)$_2$(μ_2-**L**)]·¾H$_2$O, **9**: Mp >330 °C (dec.). *m/z* (+ve mode) 532.8 ([Pd$_2$Cl$_2$(**L**-H)]$^+$, 57%); (-ve mode) 564.6 ([Pd$_2$Cl$_3$(**L**-2H)]$^-$, 100%),. Compound **9** was not obtained in sufficient quantities for further analysis.

Method B: A solution of L (12.6 mg, 0.051 mmol) was dissolved in CH$_2$Cl$_2$ (3 mL), carefully layered with THF (3 mL) and then a solution of [PdCl$_2$(PhCN)$_2$] (40.6 mg, 0.106 mmol) dissolved in toluene (3 mL). After several days a mixture of yellow rod-shaped crystals and yellow precipitate was obtained. The combined solid was collected, washed with diethyl ether (5 mL) and dried to give **8b** (21.3 mg, 82%). [PdCl$_2$(L)]·CH$_2$Cl$_2$, **8b**: Mp >290 °C (dec.). Anal. found: C, 37.78; H, 2.52; N, 15.54. C$_{14.33}$H$_{11.67}$N$_5$Cl$_{2.67}$Pd requires C, 37.84; H, 2.59; N, 15.40%. ^{1}H NMR (300 MHz; DMSO-d$_6$) δ = 5.85 (1.2H, s, ~0.6CH$_2$Cl$_2$), 7.38 (1H, t, pymH4), 7.72 (2H, dd, pyH5), 8.18 (2H, d, pyH3), 8.35 (2H, dd, pyH4), 8.74 (2H, d, pymH3/H5), 8.87 (2H, d, pyH6). Selected IR bands (ATR, cm^{-1}): 3075 (w), 1598 (m), 1559 (m), 1481 (m), 1466 (m), 1402 (vs), 1362 (w), 1331 (w), 1294 (w), 779 (m), 754 (m).

X-Ray crystallography

Crystals were mounted under oil on nylon loops. X-ray diffraction data were collected with Mo-Kα radiation (λ = 0.71073 Å) using a Bruker-AXS Single Crystal Diffraction System fitted with an Apex II CCD detector at 110(2) K (structure **6**), or an Oxford Diffraction X-calibur single crystal X-ray diffractometer at 150(2) K (structures **5LT**, **5RT**, **8b**, **9**). The structure of compound **7** was collected with Cu-Kα radiation (λ = 1.54184 Å) using an Oxford Diffraction X-calibur Sapphire 3 single crystal X-ray diffractometer at 150(2) K. Data sets were corrected for absorption using a multi-scan method, and structures were solved by direct methods using SHELXS-97[36] and refined by full-matrix least squares on F^2 by SHELXL-97,[37] interfaced through the program X-Seed.[38] In general, all non-hydrogen atoms were refined anisotropically and hydrogen atoms were included as

invariants at geometrically estimated positions, unless specified otherwise in additional details below. Figures were produced using the program POV-Ray,[39] interfaced through X-Seed. Publication materials were prepared using CIFTAB.[40] Details of data collections and structure refinements are given below and in Table 1. CCDC 860850 - 860855 contain the supplementary crystallographic data for these structures. These data can be obtained free of charge from The Cambridge Crystallographic Data Centre via www.ccdc.cam.ac.uk/data_request/cif.

Specific details of the structure refinements

Compound 6: The hexafluorophosphate anion of compound **6** is disordered over two positions with an 83:17 ratio of occupancies.

Compound 9: The hydrogen atoms of the two water molecules lying on special positions in the structure of **9** were not located (1½H atoms per asymmetric unit).

Table 1. Crystal data and X-ray experimental data for **5–9**.

Compound	5RT	5LT	6	7	8b	9
Empirical formula	$C_{15}H_{11}Fe_{0.5}N_6S$	$C_{15}H_{11}Fe_{0.5}N_6S$	$C_{28}H_{22}AgF_6N_{10}P$	$C_{29}H_{29}B_2CuF_8N_{10}O_3$	$C_{15}H_{13}Cl_4N_5Pd$	$C_{14}H_{12.5}Cl_4N_5O_{0.75}Pd_2$
Formula weight	335.29	335.29	751.40	802.78	511.50	617.39
Crystal system	triclinic	triclinic	triclinic	monoclinic	monoclinic	monoclinic
Space group	P-1	P-1	P-1	$P2_1/c$	$P2_1/n$	$C2/c$
a (Å)	8.6951(5)	8.3568(6)	10.4906(11)	19.0488(15)	10.1517(5)	23.206(2)
b (Å)	8.7849(5)	8.6842(6)	10.9594(10)	12.1691(6)	13.9219(9)	13.0040(4)
c (Å)	10.4062(5)	10.4787(7)	13.6662(14)	16.1962(12)	13.3483(8)	18.1675(16)
α (°)	88.082(4)	87.314(5)	75.933(8)	90	90	90
β (°)	80.082(4)	80.761(6)	71.510(9)	113.689(9)	89.253(5)	136.070(16)
γ (°)	79.888(5)	78.298(6)	82.371(8)	90	90	90
Volume ($Å^3$)	770.84(7)	734.92(9)	1442.8(2)	3438.0(4)	1886.37(19)	3803.7(5)
Z	2	2	2	4	4	8
Density (calculated) (Mg/m^3)	1.445	1.515	1.730	1.551	1.801	2.156
Absorption coefficient (mm^{-1})	0.668	0.700	0.833	1.723	1.559	2.466
F(000)	344	344	752	1632	1008	2380
Crystal size (mm^3)	0.26x0.15x0.04	0.20x0.15x0.05	0.46x0.24x0.23	0.17x0.16x0.13	0.29x0.19x0.04	0.16x0.09x0.04
Theta range (°)	2.35 – 30.07	2.40 – 29.82	1.61 – 39.49	4.70 – 71.29	2.48 to 26.37	2.53 – 29.21
Reflections collected	13358	10723	59552	11958	11620	17661
Observed reflections [I>2σ(I)]	4048	3816	15838	6396	3693	4520
Goodness-of-fit on F^2	0.773	0.898	1.187	0.942	1.063	1.060
R_1 [I>2σ(I)]	0.0370	0.0340	0.0360	0.0560	0.0327	0.0339
wR_2 (all data)	0.0684	0.0676	0.1191	0.1565	0.0820	0.0775

Accessory publications

^{1}H NMR spectra for complexes **6, 8a**, and **8b**, and cifs for complexes **5-9** are available from the journal's website.

References

[1]   K. S. Murray, *Eur. J. Inorg. Chem.* **2008**, 3101.

[2]   S. Hayami, Y. Komatsu, T. Shimizu, H. Kamihata, Y. H. Lee, *Coord. Chem. Rev.* **2011**, *255*, 1981.

[3]   M. A. Halcrow, *Chem. Soc. Rev.* **2011**, *40*, 4119.

[4]   J. Olguin, S. Brooker, *Coord. Chem. Rev.* **2011**, *255*, 203.

[5]   C. Atmani, F. El Hajj, S. Benmansour, M. Marchivie, S. Triki, F. Conan, V. Patinec, H. Handel, G. Dupouy, C. J. Gomez-Garcia, *Coord. Chem. Rev.* **2010**, *254*, 1559.

[6]   M. A. Halcrow, *Coord. Chem. Rev.* **2009**, *253*, 2493.

[7]   K. S. Murray, *Aust. J. Chem.* **2009**, *62*, 1081.

[8]   S. Brooker, J. A. Kitchen, *Dalton Trans.* **2009**, 7331.

[9]   V. Balzani, A. Juris, M. Venturi, S. Campagna, S. Serroni, *Chem. Rev.* **1996**, *96*, 759.

[10] J. A. Real, A. B. Gaspar, V. Niel, M. C. Munoz, *Coord. Chem. Rev.* **2003**, *236*, 121.

[11]   J. A. Real, I. Castro, A. Bousseksou, M. Verdaguer, R. Burriel, J. Linares, F. Varret, *Inorg. Chem.* **1997**, *36*, 455.

[12]   C. Kaes, A. Katz, M. W. Hosseini, *Chem. Rev.* **2000**, *100*, 3553.

[13]   C. J. Sumby, *Coord. Chem. Rev.* **2011**, *255*, 1937.

[14]   W. M. Bloch, C. J. Sumby, *Chem. Comm.* **2012**, *48*, 2534.

[15]   J. J. M. Amoore, C. J. Kepert, J. D. Cashion, B. Moubaraki, S. M. Neville, K. S. Murray, *Chem., Eur. J.* **2006**, *12*, 8220.

[16]   J. J. M. Amoore, S. M. Neville, B. Moubaraki, S. S. Iremonger, K. S. Murray, J.-F. Letard, C. J. Kepert, *Chem., Eur. J.* **2010**, *16*, 1973.

[17]   C. J. Sumby, B. A. Leita, B. Moubaraki, K. S. Murray, P. J. Steel, *Aust. J. Chem.* **2009**, *62*, 1142.

[18]   S. M. Neville, B. A. Leita, G. J. Halder, C. J. Kepert, B. Moubaraki, J.-F. Letard, K. S. Murray, *Chem., Eur. J.* **2008**, *14*, 10123.

[19]   S. M. Neville, B. A. Leita, D. A. Offerman, M. B. Duriska, B. Moubaraki, K. W. Chapman, G. J. Halder, K. S. Murray, *Eur. J. Inorg. Chem.* **2007**, 1073.

[20]   M. Quesada, V. A. de la Pena-O'Shea, G. Aromi, S. Geremia, C. Massera, O. Roubeau, P. Gamez, J. Reedijk, *Adv. Mater.* **2007**, *19*, 1397.

[21]   M. Quesada, M. Monrabal, G. Aromi, V. A. de la Pena-O'Shea, M. Gich, E. Molins, O. Roubeau, S. J. Teat, E. J. MacLean, P. Gamez, J. Reedijk, *J. Mat. Chem.* **2006**, *16*, 2669.

[22]   M. Quesada, P. de Hoog, P. Gamez, O. Roubeau, G. Aromi, B. Donnadieu, C. Massera, M. Lutz, A. L. Spek, J. Reedijk, *Eur. J. Inorg. Chem.* **2006**, 1353.

[23]   T. M. Ross, B. Moubaraki, K. S. Wallwork, S. R. Batten, K. S. Murray, *Dalton Trans.* **2011**, *40*, 10147

[24] T. M. Ross, B. Moubaraki, S. M. Neville, S. R. Batten, K. S. Murray, *Dalton Trans.* **2012**, *41*, 1512.

[25] K. K. Mosny, R. H. Crabtree, *Inorg. Chim. Acta* **1996**, *247*, 93.

[26] P. Gütlich, H. A. Goodwin (Eds.), *Top. Curr. Chem.* **2004**, *233–235*.

[27] C. Janiak, *J. Chem. Soc., Dalton Trans.* **2000**, 3885.

[28] G. R. Desiraju, T. Steiner, *The Weak Hydrogen Bond in Structural Chemistry and Biology*, Oxford University Press, **1999**.

[29] M. Domagała, S. J. Grabowski, K. Urbaniak, G. Mlostoń, *J. Phys. Chem. A* **2003**, *107*, 2730.

[30] B. Antonioli, D. J. Bray, J. K. Clegg, K. Gloe, K. Gloe, O. Kataeva, L. F. Lindoy, J. C. McMurtrie, P. J. Steel, C. J. Sumby, M. Wenzel, *Dalton Trans.* **2006**, 4783.

[31] C. J. Sumby, P. J. Steel, *Inorg. Chim. Acta* **2007**, *360*, 2100.

[32] A. W. Addison, T. N. Rao, J. Reedijk, J. Vanrijn, G. C. Verschoor, *J. Chem. Soc., Dalton Trans.* **1984**, 1349.

[33] C. J. Sumby, P. J. Steel, *J. Coord. Chem.* **2008**, *61*, 117.

[34] R. L. Martin, A. H. White, *Trans. Metal. Chem.* **1968**, *4*, 113.

[35] M. S. Kharasch, R. C. Seyler, F. R. Mayo, *J. Am. Chem. Soc.* **1938**, *60*, 882.

[36] G. M. Sheldrick, *Acta Cryst.* **1990**, *A46*, 467.

[37] G. M. Sheldrick, *SHELXL-97*, University of Göttingen, Göttingen, Germany, **1997**.

[38] L. J. Barbour, *J. Supramol. Chem.* **2001**, *1*, 189.

[39] Persistence of Vision Raytracer Pty. Ltd, *POV-Ray*, Williamstown, Australia, **2003-2008**.

[40] G. M. Sheldrick, *CIFTAB*, University of Göttingen, Göttingen, Germany, **1997**.